

Raman spectrum of solid hydrogen deuteride

J. J. Miller, R. L. Brooks, and J. L. Hunt

University of Guelph, Guelph, Ontario, Canada N1G 2W1

(Received 21 January 1993)

A Raman spectrometer using a focused laser beam and an external resonator was designed and built to study solid hydrogen samples using Raman scattering. A number of transitions were observed in the spectrum of solid HD, including an $R_0(0)$ ($\Delta J=1$) and a $T_0(0)+S_0(0)$ ($\Delta J_1=3, \Delta J_2=2$) transition. The intensity of the latter was 4.4×10^{-6} relative to the allowed $S_0(0)$ line. These transitions occur in HD as a result of the shifted components of the induced polarizability, which arise because of the separation between the center of mass and center of interaction in a HD molecule. Theoretical intensity calculations of both transitions are in very good agreement with measured intensities. A $U_0(0)$ ($\Delta J=4$) and $U_0(0)+S_0(0)$ transition were also observed, but calculations show that the induced polarizability makes a negligible contribution to both transitions. A feature in the vibrational (0-1) band was observed near the expected position of the $R_1(0)$ transition, but disagreement between the measured and theoretical intensity and a frequency 7 cm^{-1} higher than measured in absorption experiments led to its identification as part of the Q_R phonon band. The observed Q_R phonon then appeared very similar to the same feature observed in absorption: a multicomponent peak, followed by a dip in intensity, followed by another peak. R_R phonon bands associated with the $R_0(0)$ and $R_1(0)$ transitions were also observed with intensities much greater than the zero-phonon lines. Two larger features in the low-frequency wings of the $S_0(0)$ and $S_1(0)$ lines were observed and evidence was presented for the identification of these features as extensions of the R_R phonon bands, giving the R_R phonons a similar appearance to the Q_R phonon.

I. INTRODUCTION

The Raman spectrum of a gas of diatomic molecules such as H_2 is restricted by the symmetry of the molecular polarizability to transitions obeying the rotational selection rule $\Delta J=0, \pm 2$, where J is the rotational-angular-momentum quantum number.¹ This selection rule applies to all diatomic molecules in a state with zero electronic angular momentum, as well as to collision-induced absorption (CIA), where a transient dipole is induced in one molecule by the quadrupole moment of a collision partner. When hydrogen is studied in the condensed phases (and in the gas phase at high pressures), however, much weaker features satisfying different selection rules appear as the result of higher-order multipolar induction. The increasing sensitivity of infrared-absorption experiments has led to the observation of hexadecapole-induced $\Delta J=4$ rotational transitions, first in gaseous H_2 (Refs. 2,3) and later in liquid and solid H_2 (Refs. 4,5), D_2 (Refs. 6,7), and HD.⁸ More recently, Okumura *et al.*⁹ and Chan *et al.*¹⁰ have observed the 64-pole-induced $\Delta J=6$ transition in solid H_2 .¹¹ Similar interaction-induced effects have also been seen in the Raman spectrum of solid hydrogen. Using laser excitation, Prior and Allin were able to observe for the first time a number of double transitions in solid H_2 and D_2 .¹² These transitions included a broad $Q_1(0)+S_0(0)$ line along with several double rotational lines of the type $S_0(0)+S_0(J)$, and were caused by the simultaneous excitation of two molecules in a single-scattering event. In the notation used here, the

letters Q, R, S , etc. correspond to rotational transitions with $\Delta J=J'-J''=0, 1, 2$, etc., where J'' is the rotational-angular momentum of the lower state and J' is that of the upper state. The rotational quantum number of the lower state J'' is given in parentheses, and the subscript indicates the vibrational quantum number v' of the upper state.

Transitions involving a change in total rotational-angular momentum greater than two were also seen by Berkhout and Silvera, who published the first spectra showing the double- S Raman transitions in pressurized solid H_2 and D_2 .¹³ A $U_0(0)$ transition corresponding to $\Delta J=4$ and a $U_0(0)+S_0(0)$ double rotational transition were also reportedly observed, although a single line due to $U_0(0)$ did not appear resolved from the broader, more intense $S_0(1)+S_0(1)$ double transition. Two mechanisms can contribute to these forbidden transitions in the Raman spectrum: mixing of rotational states by the electric quadrupole-quadrupole (EQQ) interaction, and the breakdown of the independent polarizability approximation (BIPA). The dependence of the scattered light intensity on the density of the solid was shown to be different for the two mechanisms, and a comparison of the calculated intensity with measurements made as a function of pressure up to 2 kbar on the $S_0(1)+S_0(1)$ transition showed very good agreement.¹³ More recently, double transitions of the type $Q_1(0)+S_0(0)$ in the vibrational band have been reexamined in both solid H_2 (Ref. 14) and D_2 (Ref. 6). Whereas the contributions to the $S_0(J_1)+S_0(J_2)$ intensities from the two mechanisms of state mixing and

BIPA are comparable,¹³ Barocchi *et al.* have shown that the BIPA is insignificant in accounting for the $Q_1(0)+S_0(0)$ intensity.¹⁴ The reason state mixing is such a dominant effect is that the energy difference between the $S_1(0)$ and the $Q_1(0)+S_0(0)$ states (6 cm^{-1} in D_2 and 18 cm^{-1} in H_2) is much less than the energy separation between different rotational levels, and is of the same order of magnitude as the EQQ interaction coupling these different states. Using perturbation theory and considering only state mixing due to the EQQ interaction, the intensity of the double transition $Q_1(0)+S_0(0)$ was calculated to be about 0.2 times that of the allowed $S_1(0)$ line, which agreed to within experimental uncertainty with the measured double transition intensity.¹⁴

Unlike H_2 or D_2 , the HD molecule possesses a small, permanent dipole moment, allowing normal absorption transitions with $\Delta J = +1$ to be observed in the low-pressure gas¹⁵ as well as in the solid. The $R_0(0)$ line, first observed in solid H_2 by Treffer *et al.*,¹⁶ has recently been remeasured in two separate experiments^{17,18} and its intensity has been found to agree well with a recent *ab initio* calculation by Tipping and Poll.¹⁹ Only about half of the $R_0(0)$ intensity, however, is caused by the allowed dipole moment. The remaining intensity arises because of the so-called "shifted components" of the induced dipole moments as well as constructive interference between the allowed and induced moments. The origin of these shifted components has been discussed previously.²⁰ In HD the center of mass does not coincide with the center of charge, and when the coordinate transformation from the center of charge to the center of mass is made, the various interaction-induced dipoles give rise to additional shifted components with different symmetry properties from the unshifted dipoles. In contrast to the $R_0(0)$ line, the allowed dipole moment does not contribute significantly to the $R_1(0)$ absorption line in the fundamental (0-1) vibrational band, leaving the induced dipole and interference between the allowed and induced dipoles to account for the observed transition intensity.²¹ Other transitions having odd values of ΔJ greater than one can also occur in solid HD, although not in H_2 or D_2 . These transitions are also the result of the separation of the center of mass from the center of charge of the molecule. For example, the quadrupole-induced dipole moment gives rise under a coordinate transformation to additional shifted dipole components that contribute to the $T_{v'}(0)$ single transition as well as the $S_{v'}(0)+R_{v'}(0)$ and $S_{v'}(0)+T_{v'}(0)$ double transitions. Similarly, the hexadecapole-induced dipole, when shifted, gives contributions to the $V_{v'}(0)$ single transition corresponding to $\Delta J = +5$. Several such absorption transitions have already been observed in solid HD²² and the measured absorption coefficients have been compared with theoretical values obtained using *ab initio* matrix elements.²³

Like the induced dipole moment, the interaction-induced polarizability in solid HD also contains shifted components due to the separation between the center of charge and the center of mass, leading to rotational Raman transitions with odd values of ΔJ . The occurrence of these normally forbidden transitions in the Raman

spectrum was first predicted by Attia *et al.*²⁴ who also calculated several transition intensities. The calculated intensities were not large; the strongest, $R_0(0)$, was predicted to be only 1.8×10^{-4} times as intense as the allowed $S_0(0)$ transition, although the accompanying phonon branch was predicted to be 15 times stronger than $R_0(0)$. In order to test these predictions, the Raman spectrum of solid HD has been reexamined under high sensitivity, and we are able to report the observation of such transitions having odd values of ΔJ , including $R_0(0)$ and an accompanying phonon branch, as well as the double transition $T_0(0)+S_0(0)$. While neither of these zero-phonon lines has been observed before, it was suggested by Attia *et al.*²⁴ that a broad peak in the rotational Raman spectrum of solid HD, previously observed by Silvera *et al.* and identified as two-phonon scattering,²⁵ may have actually been the phonon branch accompanying the $R_0(0)$ transition. Silvera *et al.* recognized the possibility, in principle, of a $\Delta J = +1$ transition occurring in the HD spectrum, but having not observed the single transition it was considered more likely that the broad peak at $\sim 160\text{ cm}^{-1}$ was caused by two-phonon scattering.²⁵ The issue of the identity of this feature will be readdressed in this article. In addition to the odd ΔJ lines, a sharp $U_0(0)$ line corresponding to $\Delta J = 4$ transitions in single molecules and a $U_0(0)+S_0(0)$ double transition have also been observed. The occurrence of these new transitions in the Raman spectrum of solid HD affords a unique opportunity to investigate the effects of intermolecular interactions using a well-established experimental technique.

II. THEORY

The theory of Raman transitions in solid HD with odd values of ΔJ has been presented previously by Attia *et al.*²⁴ along with intensity calculations of the $R_v(0)$, $R_v(0)+S_{v'}(0)$, and $T_{v'}(0)+S_{v'}(0)$ transitions and their associated phonon branches in the rotational band ($v=v'=0$). Their calculations were for the case of a single oriented crystal with its c axis in the laboratory-frame Z direction, the laser beam also along the Z direction with X polarization, and the scattered light along the X direction with Y and Z polarization. A shorthand method of referring to this combination of polarizations is $XY+XZ$, where the first letter of a pair gives the laser beam polarization referred to a laboratory-fixed coordinate system and the second letter gives the scattered light polarization. In the experiments reported here, the laser beam was polarized along the Y direction, so the polarization geometry was $YY+YZ$. The geometry of the experiment is illustrated in Fig. 1.

In the independent polarizability approximation, the polarizability of an assembly of molecules is just equal to the sum of the individual molecular polarizabilities. When interactions between molecules are considered, the total polarizability will include additional induced components. For a pair of interacting hydrogen molecules, a component of the polarizability tensor can be written²⁴

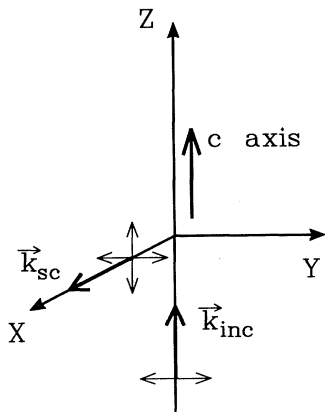


FIG. 1. Scattering geometry used in the Raman experiments on solid HD. The incident laser light is along the laboratory-fixed Z axis with polarization along Y, and the scattered light is in the X direction with polarization along both Y and Z. The sample is assumed to be a single oriented crystal with c axis along the Z direction.

$$\alpha_{\lambda\mu}(\mathbf{r}_1\mathbf{r}_2\mathbf{R}) = \alpha_{\lambda\mu}(\mathbf{r}_1) + \alpha_{\lambda\mu}(\mathbf{r}_2) + \alpha_{\lambda\mu}^{\text{ind}}(\mathbf{r}_1\mathbf{r}_2\mathbf{R}), \quad (1)$$

where $\alpha_{\lambda\mu}(\mathbf{r}_i)$ is the polarizability of an isolated molecule and $\alpha_{\lambda\mu}^{\text{ind}}(\mathbf{r}_1\mathbf{r}_2\mathbf{R})$ is the interaction-induced pair polarizability. The vectors $\mathbf{r} = (r_i, \omega_i)$ are the internuclear separations of the molecules referred to a laboratory-fixed coordinate system, with $\omega_i \equiv (\theta_i, \phi_i)$ giving the orientation. Similarly, $\mathbf{R} = (R, \Omega)$ is the vector between the centers of mass of the two molecules. The pair polarizability $\alpha_{\lambda\mu}^{\text{ind}}(\mathbf{r}_1\mathbf{r}_2\mathbf{R})$ contributes to the double rotational Raman transitions $S_0(J) + S_0(J')$ in H_2 , D_2 , and HD.

Like a pair of H_2 molecules, the interaction-induced polarizability for a pair of HD molecules is a function of the internuclear separations \mathbf{r}_i and the vector between the centers of interaction of the two molecules. The difference is that this vector does not coincide with the vector separation between the centers of mass, as it does for a pair of H_2 molecules. If the vector from the internuclear midpoint of a molecule labeled i to the center of mass is called \mathbf{x}_i , then $\mathbf{x}_i = \mathbf{r}_i/6$ for an HD molecule. If the vector between the centers of interaction of the two molecules is now called \mathbf{S} , then

$$\mathbf{S} = \mathbf{R} + (\mathbf{x}_1 - \mathbf{x}_2), \quad (2)$$

where \mathbf{R} is still the vector between the centers of mass. In order to calculate matrix elements of $\alpha_{\lambda\mu}^{\text{ind}}(\mathbf{r}_1\mathbf{r}_2\mathbf{S})$ for a pair of HD molecules, the induced polarizability must first be expressed in terms of the appropriate dynamical variables $(\mathbf{r}_1\mathbf{r}_2\mathbf{R})$,²⁶ since the rotational wave functions are referred to the molecular centers of mass. This transformation can be made with the help of Eq. (2) to give the following Taylor series:²⁴

$$\alpha_{\lambda\mu}^{\text{ind}}(\mathbf{r}_1\mathbf{r}_2\mathbf{S}) = \alpha_{\lambda\mu}^{\text{ind}}(\mathbf{r}_1\mathbf{r}_2\mathbf{R}) + (\mathbf{x}_1 - \mathbf{x}_2) \cdot \nabla_{\mathbf{R}} \alpha_{\lambda\mu}^{\text{ind}}(\mathbf{r}_1\mathbf{r}_2\mathbf{R}) + \dots \quad (3)$$

The first term in Eq. (3) is just the interaction-induced po-

larizability given by Eq. (1) for a pair of H_2 molecules. It is the second term proportional to \mathbf{x}_1 and \mathbf{x}_2 in the expansion (3) that contains the shifted polarizability components; these have different symmetries from the unshifted components and give rise to single $R_v(0)$ transitions and double transitions such as $R_v(0) + S_{v'}(0)$ and $T_v(0) + S_{v'}(0)$.

The intensities of these transitions in the rotational Raman spectrum calculated within the dipole-induced dipole model by Attia *et al.*²⁴ range from 1.8×10^{-4} for $R_0(0)$ to 4.2×10^{-6} for $T_0(0) + S_0(0)$. All intensities are given relative to the allowed (HD) $S_0(0)$ line. The calculations have been repeated for the single and double molecule transitions for the different laser beam polarizations used in these experiments, and the intensities were found to be only slightly different, ranging from 1.5×10^{-4} for $R_0(0)$ to 4.8×10^{-6} for $T_0(0) + S_0(0)$.²⁷ Intensities for the accompanying phonon bands have not been recalculated for the present case, but they should not differ appreciably from the results of Ref. 24. The phonon branches associated with the double transitions were calculated to be approximately half as intense, but for the $R_0(0)$ line, the accompanying phonon branch, commonly denoted by the notation R_R , was predicted to be 15 times as intense as the single molecule transition.²⁴

III. EXPERIMENTAL DETAILS

The usual 90° scattering geometry depicted in Fig. 1 was used, along with the standard photon counting mode of detection. A beam from an argon-ion laser with a maximum power of approximately $\frac{3}{4}$ W was passed vertically through the sample. A 101 mm focal length best-form lens placed below the cell focused the beam to a spot size of 17 μm at the sample center. After passing through the cell, a 230 mm spherical mirror mounted on a micrometer-adjustable translation stage reflected the beam back on itself. Careful positioning of this mirror produced an external resonating cavity that increased the laser beam power inside the sample by a factor of between 4 and 10, depending on sample transparency and reflection losses from windows and other optical components. The scattered light was collected and focused onto the entrance slit of a Spex 1400-II double monochromator, and detected by an EMI 9865 photomultiplier tube mounted at the exit slit. The entire light collection system, including the monochromator and detector, was calibrated for frequency response by recording the spectrum of a quartz halogen lamp that had itself been calibrated against an Optronic Laboratory model 200C standard lamp. The spectral irradiance of this lamp was known between 375 and 800 nm with an uncertainty of $\pm 1.4\%$ from comparison with a National Institute of Standards and Technology standard lamp.

The sample cell was constructed of copper with an interior volume of approximately 1 cm^3 and was similar in design to cells used in previous experiments.^{28,29} The bottom of the cell was mounted to a copper bracket connected to the cold finger of a Janis Research ST transfer line cryostat, and the entire cell-cold finger assembly was sealed inside an evacuated aluminum shroud. Liquid

helium was used to cool the cell down to around 15 K, the lowest temperature used when recording solid spectra. A Lakeshore Cryotronics DRC-80 temperature controller monitored the temperature of the cell to within 0.1° and allowed the temperature to be controlled by a wire heater wrapped around the cold finger. A second 0.5 W wire heater on the top of the cell provided localized heating at the point where the stainless-steel gas line entered the cell. This auxiliary heater fulfilled two functions. First, it prevented the gas inlet line from freezing shut before the contents of the cell had completely frozen. Second, by heating the cell on top and cooling it from the bottom, the thermal gradient inside the cell was predominantly vertical; this was essential to establish a preferred orientation for the c axes of the crystals during the freeze.

The HD gas used was purchased from MSD Isotopes. Before it could be used, the gas first had to be distilled to remove considerable air impurities. Even then, the gas typically was a mixture of 5% H_2 :90% HD:5% D_2 . Crystals were grown by first pressurizing the cell filled with liquid HD to between 300 and 400 psi, then very gradually decreasing the temperature (about 0.1° every twenty min) until the sample was completely frozen. Once frozen, the solid samples contained no obvious visual flaws, although observation between two polarizers revealed many grain boundaries, confirming that the sample was polycrystalline. The actual orientations of the crystallites is uncertain but must lie somewhere between a uniform vertical alignment and a completely random distribution. Theoretical intensities were calculated for both of these limiting possibilities, and the results will be discussed in Sec. V.

IV. RESULTS

A. The rotational band

The rotational Raman spectrum of solid HD is shown in Fig. 2. The horizontal axis gives the frequency shift from the laser line in wave numbers, and the spectral resolution is 2 cm^{-1} . On the intensity scale used for the spectrum in Fig. 2(a), only the normally Raman allowed features satisfying $\Delta J=2$ can be seen. The largest line is the allowed $S_0(0)$ transition in HD, but there are also four additional $S_0(J)$ transitions with $J=0$ and 1 due to the presence of H_2 and D_2 in the sample. From the measured relative intensities of these lines, the concentration of both H_2 and D_2 in the sample is estimated to be 5% each. While the linewidths (full width at half maximum) of the H_2 and $D_2 S_0(J)$ lines were found to vary from 2.2 to 4.9 cm^{-1} , the width of the HD $S_0(0)$ line was measured to be 9 cm^{-1} , or two to four times larger than any of the other lines. This large difference in linewidth was first noticed by McTague *et al.*³⁰ who showed that the HD $S_0(0)$ line, like the $S_0(0)$ lines in H_2 and D_2 , also consisted of three components, but that each of these components in HD had full widths at half maximum (FWHM) of 5.5 to 6 cm^{-1} and appeared to be lifetime broadened. By measuring the polarization characteristics of the $S_0(0)$ line in single crystals of solid HD, McTague

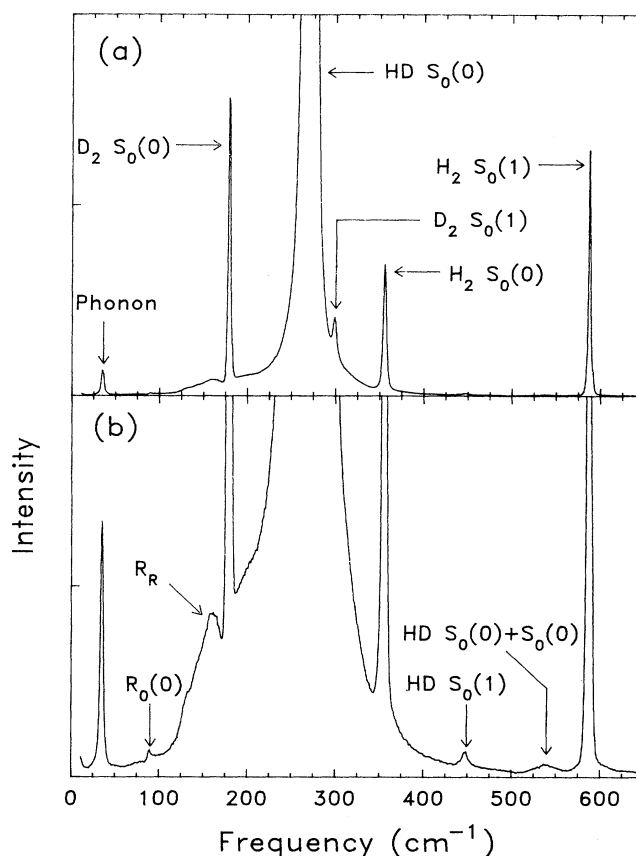


FIG. 2. The rotational Raman spectrum of solid HD at 15 K. The horizontal axis gives the frequency shift in wave numbers from the laser light frequency. Both spectra are identical, but the intensity scale in (b) is expanded by a factor of 10.

et al. unambiguously identified the three components as transitions to the $m = \pm 1$ (lowest energy), $m = \pm 2$, and $m = 0$ (highest energy) levels in the $J=2$ roton band.³⁰ The degeneracy of the m_J sublevels is removed by the mainly anisotropic EQQ interactions. The use of three Lorentzian line shapes to model the HD $S_0(0)$ line also proved to be successful for the spectra shown here, as will be discussed shortly.

Another fairly prominent feature that can still be seen with the intensity scale used in Fig. 2(a) is the pure phonon line at 35.2 cm^{-1} . This line represents the transverse-optic (TO) phonon and is also a Raman allowed transition. Silvera *et al.* first observed this line and accurately measured its frequency in H_2 , D_2 , and HD.²⁵ Their measured value of 36.16 cm^{-1} in solid HD at 4.2 K is 1 cm^{-1} higher than the value reported here for a sample at 15 K, but it was also noted that raising the temperature of a para- D_2 sample from 4.2 to 14.2 K lowered the phonon frequency by 1.8 cm^{-1} (Ref. 25). In light of this result, the measured frequency of 35.2 cm^{-1} is consistent with both the Silvera *et al.* value and the result of Baliga *et al.* of 37.0 cm^{-1} obtained with a solid temperature of 2 K.⁶

The spectrum of Fig. 2(a) is shown in Fig. 2(b) with an intensity scale ten times more sensitive, and a number of weaker features appear. The relatively narrow line at 448 cm^{-1} is the HD $S_0(1)$ transition. Even at 15.5 K, the temperature of the sample, about 7.5 HD molecules out of 10^4 are in the $J=1$ rotational level, according to the Boltzmann population distribution. The line at 538 cm^{-1} with an intensity comparable to the $S_0(1)$ line is the double transition $S_0(0)+S_0(0)$. One notable characteristic of this line is its large width; the FWHM was measured to be around 24 cm^{-1} . Such a large width is not unexpected, but rather seems to be characteristic of double transitions. The $S_0(J)+S_0(J')$ double transitions observed by Berkhout and Silvera in solid H_2 and D_2 also appeared significantly broader than the single transitions, although values of the linewidths were not quoted.¹³ In HD the apparent broadening of the Δm_J components discussed previously would also increase the linewidth of the double transition. Furthermore, it has been suggested that the forbidden transitions such as $S_0(J)+S_0(J')$ may be expected to contain relatively strong phonon sidebands.¹³ The existence of an unresolved phonon branch adjacent to the HD $S_0(0)+S_0(0)$ line might therefore also be a contributing factor to the shape and width of this line.

On the low-frequency side of the HD $S_0(0)$ line are a couple of other weaker features that can be seen in Fig. 2(b). The weak, relatively sharp line at about 90 cm^{-1} is the $R_0(0)$ transition whose occurrence in the Raman spectrum of solid HD was predicted by Attia *et al.*²⁴ A much stronger feature with a peak at about 160 cm^{-1} , just to the left of the $\text{D}_2 S_0(0)$ line, can also be seen. This feature has been identified as the phonon sideband accompanying the $R_0(0)$ transition and is labeled R_R in keeping with the established convention of designating phonon sidebands by the subscript R . The intensity of this phonon band has been calculated to be 15 times as intense as the $R_0(0)$ line.²⁴ While the calculation was done for the case of $XY+XZ$ polarization, it will be assumed that approximately the same ratio will occur for $YY+YZ$ polarization used in the present experiments. From a qualitative standpoint, therefore, the assignment of this feature as the R_R phonon sideband seems valid. But as Silvera *et al.*,²⁵ who observed the same feature in an earlier Raman spectrum of solid HD between 50 and 230 cm^{-1} , previously pointed out, two-phonon scattering is also expected to occur in this spectral region. While no predictions of the intensity of scattering by this mechanism have been made, its contribution to this part of the spectrum cannot be dismissed.

An asymmetry in the wings of the HD $S_0(0)$ line caused by a broad feature just to the high-frequency side of the $\text{D}_2 S_0(0)$ line can also be noticed in Fig. 2(b). This additional intensity, which was also observed by Silvera *et al.* but not commented upon,²⁵ may represent a contribution from two-phonon scattering. To explore this possibility, the Raman spectrum of solid H_2 was looked at between 0 and 300 cm^{-1} . Because solid hydrogen is a quantum crystal, there is only a very weak dependence of the phonon frequencies on the molecular mass, and the

single phonon frequency measured in H_2 was within 1 cm^{-1} of the corresponding frequency in HD. It can be expected that the two-phonon continuum will also be very similar in both isotopomers, however, in H_2 the only Raman-active mode between the single phonon and the $S_0(0)$ line at 354 cm^{-1} is this two-phonon excitation. The H_2 spectrum showed a broad feature that peaked between 100 and 150 cm^{-1} and then decreased gradually to zero between 250 and 300 cm^{-1} . Based on this observation, it does not seem likely that the feature seen in Fig. 2(b) with a peak around 200 cm^{-1} can be attributed to two-phonon scattering. Another possible contribution may be a phonon sideband associated with $\text{D}_2 S_0(0)$, although the absence of noticeable sidebands on most of the other $S_0(J)$ transitions suggests that this contribution would be weak at best.

The spectrum of Fig. 2 over the region from 10 to 200 cm^{-1} is shown on a more sensitive intensity scale in Fig. 3. The $R_0(0)$ line, displayed in the inset, was recorded with a resolution of 1 cm^{-1} and is seen to have a very asymmetric line shape. It is also apparent that the feature that has been identified as the R_R phonon band contains at least two components. To determine the intensities of the $R_0(0)$ and R_R features to compare with theoretical intensities required separating these features from the underlying spectrum. Both features sit on top of the wing of the intense HD $S_0(0)$ line, in addition to the two-phonon spectrum whose shape and intensity are unknown, and the currently unidentified component mentioned in the previous paragraph. To separate these various features, the wing of the HD $S_0(0)$ line was modeled first. Using three Lorentzians constrained to have equal

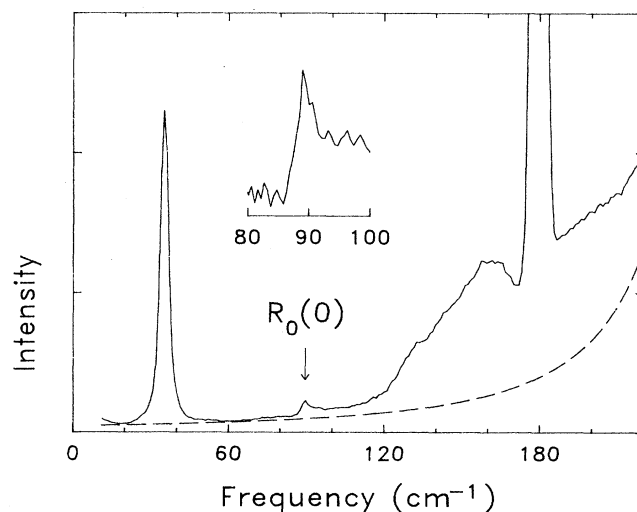


FIG. 3. The rotational Raman spectrum of solid HD on an expanded intensity scale. The $R_0(0)$ line, shown in the inset, was recorded with a spectral resolution of 1 cm^{-1} , and has a very asymmetric line shape. The dashed line represents the extrapolated wing of the large $S_0(0)$ line obtained from fitting it to three Lorentzians.

separations, it was indeed possible to fit the observed $S_0(0)$ line shape, using a nonlinear least-squares-fitting routine, out to eight or ten half-widths from the line center. By extrapolating the line shape to zero frequency using the fit parameters, a very convincing curve representing the far wing of this line was obtained, and is shown as the dashed line in Fig. 3.

Treating the wing of the HD $S_0(0)$ line as a fixed background, the remaining features were fit simultaneously using several Gaussian functions. (Gaussians were used because this function seemed to most closely match the instrumental profile, as determined from fitting gas Raman lines.) Two Gaussians were required to fit the $D_2 S_0(0)$ line, but this is not surprising given the underlying triplet structure of this line. To model the R_R feature between about 110 and 170 cm^{-1} , either two or three Gaussians were used. A final Gaussian was required to account for the shoulder to the right of the $D_2 S_0(0)$ line. Thus, by using five or six Gaussian line shapes superimposed on the HD $S_0(0)$ wing, the spectral region between 100 and 250 cm^{-1} could be modeled quite satisfactorily. The positions and integrated intensities of the components of the R_R phonon band and the unidentified feature obtained from fitting several sets of data are summarized in Table I. It will be noted that none of the components used in the fit were assigned to two-phonon scattering. Presumably, the contribution from this is lumped together with the components of the R_R phonon band. We will come back to this point a little later.

The $R_0(0)$ line was well separated from the phonon band structure and was fit independently, with the Lorentzian wing of the $S_0(0)$ line forming the background. The asymmetric line shape was modeled using the well-known Fano-type line profile, which is a characteristic feature of interference between a discrete and a continuum state.³¹ In this case the discrete state is the upper rotational level ($J=1$); the identity of the continuum is not so immediately obvious, but it is probably the two-phonon continuum which extends underneath the $R_0(0)$ line. The functional form used to fit this feature

TABLE I. Properties of the R_R phonon branch components and the unidentified phonon feature in the rotational band of solid HD as determined from least-squares fitting. The intensities are relative to the $S_0(0)$ transition.

Phonon branch components	Frequency (cm^{-1})	FWHM (cm^{-1})	Relative intensity
Two-component fit:			
R_R^a	138	21	2.0×10^{-3}
R_R^b	158	16	2.0×10^{-3}
R_R (total)			4.0×10^{-3}
Three-component fit:			
R_R^a	131	10	4.9×10^{-4}
R_R^b	148	26	3.0×10^{-3}
R_R^c	160	11	1.0×10^{-3}
R_R (total)			4.5×10^{-3}
Unknown feature	200	96	3.2×10^{-2}

was the same as that used by McKellar and Clouter to fit the same transition observed in absorption in solid HD:¹⁸

$$I(\sigma) = I_0 \frac{(1 + \epsilon/q)^2}{1 + \epsilon^2}, \quad (4)$$

where $\epsilon = 2(\sigma - \sigma_0)/\Gamma$. In Eq. (4) I_0 is the peak intensity, σ_0 is the frequency in cm^{-1} of the line, Γ is the full width at half maximum (FWHM), and q is the Fano line-shape parameter that describes the degree of asymmetry of the line. The line shape becomes more asymmetric as $|q|$ approaches zero and when $|q|$ approaches infinity, the expression (4) reduces to a symmetric Lorentzian line shape. Once the parameters in (4) were determined, the integrated intensity of the line was calculated according to¹⁸

$$I = \frac{\pi}{2} I_0 \Gamma (1 - q^{-2}). \quad (5)$$

Equation (5) is obtained from (4) by first subtracting the baseline value I_0/q^2 , which is the value $I(\sigma)$ approaches as $\sigma \rightarrow \pm\infty$, and then integrating the result from $-\infty$ to $+\infty$. Table II lists the average values of the parameters and the integrated intensity obtained after fitting four different spectra. The intensity is relative to the HD $S_0(0)$ line and has been corrected for the spectrometer response.

A number of rotational transitions were observed beyond the $H_2 S_0(1)$ line, and these are all shown in Fig. 4. This spectrum was recorded with a spectral resolution of 4 cm^{-1} . The HD $S_0(0) + S_0(0)$ and the $H_2 S_0(1)$ transitions are also included to allow for a visual comparison. Table III summarizes the measured frequencies, linewidths and integrated intensities for all of the zero-phonon transitions observed in this spectral region. No attempt has been made to correct the observed linewidths by accounting for the instrumental line shape, since most of the lines are much broader than the spectral resolution. The intensities have been corrected for the relative spectrometer response, and are given relative to the HD $S_0(0)$ line. These intensities were determined by first measuring the intensity relative to the $H_2 S_0(1)$ line, and then multiplying this ratio by the average value of the $H_2 S_0(1)$ intensity relative to HD $S_0(0)$. In this way, only lines recorded in the same spectrum under identical conditions were being compared, so that variables like the laser power, quality of the sample, etc. did not affect the comparison.

Two of the largest features shown in Fig. 4 on the $\times 40$ expanded sensitivity scale are double rotational transi-

TABLE II. Properties of the $R_0(0)$ line determined from least-squares fitting. The parameters are defined by Eq. (4) in the text. σ_0 is the line position, Γ is the linewidth (FWHM) and q is the Fano line shape parameter describing the degree of asymmetry of the line. The intensity is given relative to the $S_0(0)$ transition.

σ_0 (cm^{-1})	Γ (cm^{-1})	q	Relative intensity
88.9 ± 0.4	3.3 ± 0.8	3.9	8.5×10^{-5}

TABLE III. Raman frequencies, linewidths, and integrated intensities of zero-phonon transitions in the double rotational band of solid HD. All of the transitions are illustrated in the spectrum of Fig. 4. The integrated intensities are given relative to the $S_0(0)$ transition intensity.

Transition	Frequency (cm^{-1})	FWHM (cm^{-1})	Previous measurements	Integrated intensity
$S_0(0)+S_0(0)$	538 ± 4	24		$3.4\pm 0.3\times 10^{-4}$
$T_0(0)+S_0(0)$	807 ± 8	16	799.7 ^a	$4.4\pm 1.0\times 10^{-6}$
$(\text{HD})S_0(0)+(\text{H}_2)S_0(1)$	858 ± 4	21		$1.6\pm 0.3\times 10^{-5}$
$U_0(0)$	886.5 ± 1.5	7	885.2 ^b	$6.2\pm 0.8\times 10^{-6}$
$(\text{HD})U_0(0)+(\text{D}_2)S_0(0)$	1060 ± 2	11		$1.4\pm 1.0\times 10^{-6}$
$U_0(0)+S_0(0)$	1157 ± 4	19		$1.7\pm 0.3\times 10^{-5}$

^aReference 31; measured in absorption.

^bReference 8; measured in absorption.

tions. The one at 858 cm^{-1} involves a $\Delta J=2$ rotation occurring simultaneously in a HD and an adjacent ortho- H_2 molecule. The largest line at 1157 cm^{-1} involves HD molecules only, one making a $\Delta J=2$ transition and an adjacent molecule making a $\Delta J=4$ or U transition. A single $U_0(0)$ transition also occurs with significant intensity. The narrowness of this line is in sharp contrast to the double transitions, and once again illustrates this characteristic difference between the two types of lines. It should be noted that when the $U_0(0)$ line was recorded after reducing the slit width, the observed linewidth did not change significantly, so that the value quoted in Table III is probably close to the actual FWHM for this line. Berkhout and Silvera also reported observing single U transitions in solid H_2 and D_2 ; however, in their published spectra it is not possible to resolve a sharp line like the one observed here from the broader

$S_0(1)+S_0(1)$ transitions that occur at almost the same frequency.¹³ As a result, the spectrum of Fig. 4 probably represents an unambiguous observation of a $\Delta J=4$ Raman transition in solid hydrogen. It should also be possible to observe this transition without interference by reexamining the Raman spectrum of pure para- H_2 and ortho- D_2 .

The signal-to-noise ratio in Fig. 4 is sufficiently good to allow several other weak spectral features to be distinguished. Two of these are quite broad and have been identified as phonon sidebands. The most intense one at around 1200 cm^{-1} is labelled as $(U+S)_R$, meaning it is the phonon sideband associated with the $U_0(0)+S_0(0)$ line. An accurate measurement of the intensity of the phonons is difficult because of the width and weakness of these features, but it is estimated that the $(U+S)_R$ phonon is 0.5 ± 0.25 times the intensity of the $U_0(0)+S_0(0)$ line. The second phonon, occurring around 930 cm^{-1} , may be identified with either the HD $S_0(0)+\text{H}_2 S_0(1)$ or the $U_0(0)$ line; it is separated from these two lines by 70 and 41 cm^{-1} . In comparison, the separation between the $U_0(0)+S_0(0)$ line and its phonon is 50 cm^{-1} . There is also what appears to be a distinct phonon band associated with the $\text{H}_2 S_0(1)$ line at about 630 cm^{-1} , which is 43 cm^{-1} from the zero-phonon line. [The separation between this phonon peak and the HD $S_0(0)+S_0(0)$ transition is about 90 cm^{-1} , which is too large to make it likely that the phonon is associated with this double transition.] Based on this, it seems most likely that the phonon at 930 cm^{-1} should be identified as U_R . Its intensity is also approximately one-half that of the $U_0(0)$ line, and so it indeed appears to be the case that many of the so-called forbidden transitions have relatively large phonon sidebands. This observation also agrees generally with the theoretical results of Attia *et al.*, who calculated relative intensities of 0.54 for the phonons expected to accompany the $R_0(0)+S_0(0)$ and $T_0(0)+S_0(0)$ transitions.²⁴

Finally, and most significantly, a weak feature can be distinguished in Fig. 4 occurring at 807 cm^{-1} , and this has been identified as the $T_0(0)+S_0(0)$ double transition first predicted to occur in the Raman spectrum of solid HD by Attia *et al.*²⁴ This transition has been previously observed using infrared absorption, where its frequency was measured to be 799.7 cm^{-1} .³² This value is in sub-

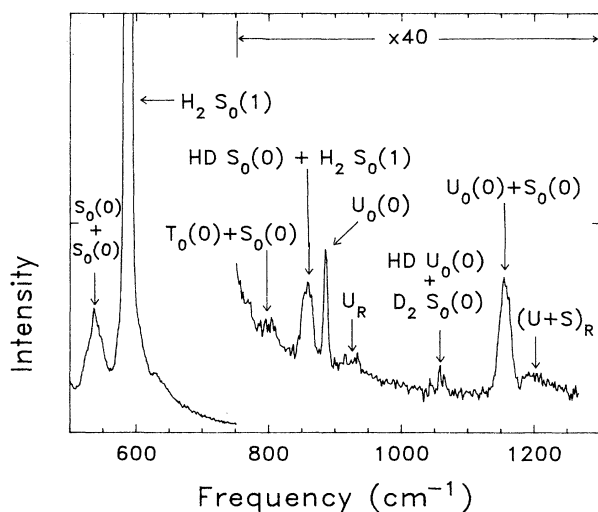


FIG. 4. The rotational Raman spectrum of solid HD showing the $U_0(0)$ transition as well as several double rotational transitions. Note that several transitions involve H_2 and D_2 molecules. The weakest features observed here are of the order of 10^{-6} times the intensity of the strong HD $S_0(0)$ transition.

stantial disagreement with the one measured here, but it still falls just within the present experimental uncertainty of $\pm 8 \text{ cm}^{-1}$. Accurate measurements of the frequency and integrated intensity of this line are hampered by its large width and weak intensity, as well as the sharply sloping background caused by the tail of the $\text{H}_2 S_0(1)$ line and its phonon band. By fitting this background to an exponential function and the $T_0(0)+S_0(0)$ line to a single Gaussian, the integrated intensity of this line relative to the HD $S_0(0)$ was determined to be 4.4×10^{-6} after correcting for the spectrometer response. This turns out to be in excellent agreement with the theoretical value, as will be discussed further in Sec. V.

B. The vibrational band

A Raman spectrum of the vibrational band of solid HD is shown in Fig. 5. The most intense line, the pure vibrational $Q_1(0)$ transition, is very narrow; its measured FWHM of 2 cm^{-1} represents the inherent instrumental linewidth. As Table IV shows, the measured frequency of 3621.7 cm^{-1} is within 0.15 cm^{-1} of previously measured values.^{18,33} The rotational vibrational transition $S_1(0)$ is a little more interesting. In addition to a symmetric main peak, it has a very noticeable component on the high-frequency side. Recent observations of the $S_1(0)$ line in solid normal D_2 (Ref. 6) and in para- H_2 (Ref. 14) have shown a similar asymmetric structure for the $S_1(0)$ line in these solids as well. The additional high-frequency component has been shown to be the double transition $Q_1(0)+S_0(0)$. According to gas phase measurements, the difference in frequency between the two different states for HD is 11.3 cm^{-1} . The asymmetric line shape shown in Fig. 5 was best fit using two components: a Lorentzian was used for the single $S_1(0)$ transition and a

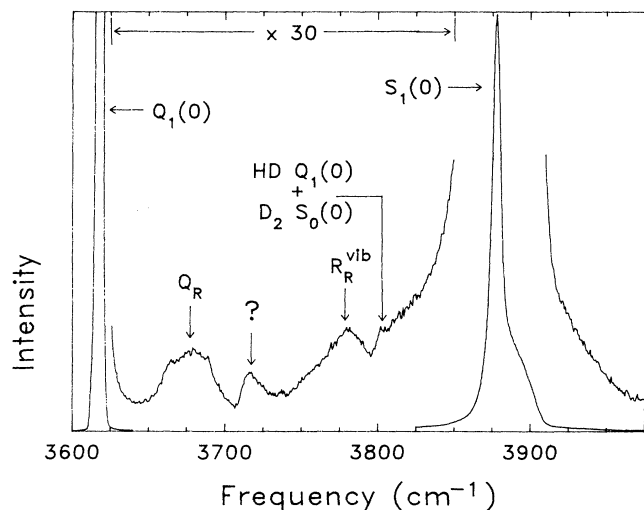


FIG. 5. The fundamental vibrational Raman spectrum of solid HD at 15 K. The asymmetry in the high-frequency wing of the $S_1(0)$ line is caused by the $Q_1(0)+S_0(0)$ double transition. Note the much weaker asymmetry in the left wing of the $S_1(0)$ line and visible only on the $\times 30$ scale.

TABLE IV. Frequencies and linewidths of zero-phonon Raman transitions in the fundamental vibrational band of solid HD. The width quoted for the $Q_1(0)$ line is the instrumental slit width; the actual linewidth is probably much narrower.

Line	Frequency (cm^{-1})	FWHM (cm^{-1})	Previous measurements
$Q_1(0)$	3621.7 ± 0.4	2	3621.85^a ; 3624.86^b
$S_1(0)$	3880.4 ± 1.0	7	3880.0^c
$Q_1(0)+S_0(0)$	3896 ± 4	17	3890^b

^aBhatnagar *et al.*, Reference 32.

^bMcKellar and Clouter, Reference 18; measured in absorption.

^cBaliga *et al.*, Reference 6.

Gaussian for the double transition. The average results after fitting several sets of data are listed in Table IV. The frequency determined for the $S_1(0)$ component agrees to within 0.4 cm^{-1} with a previous measurement,⁶ but the Gaussian component is 15 cm^{-1} higher than the $S_1(0)$ component and 5 or 6 cm^{-1} higher than the frequency of the $Q_1(0)+S_0(0)$ transition measured in absorption.¹⁸ This discrepancy simply reflects the uncertainty involved in separating the two overlapping components, and does not cast any doubt on the origin of the asymmetry in the $S_1(0)$ line.

The intensity of the $Q_1(0)+S_0(0)$ transition relative to the $S_1(0)$ was determined to be 0.21, however, this value has an uncertainty of about 10% for reasons already discussed. Barocchi *et al.*¹⁴ have discussed the theory of this double transition and have shown that it is caused mainly by mixing of the unperturbed states by the electric quadrupole-quadrupole (EQQ) interaction. (The interaction-induced polarizability also makes a contribution, but this is negligible compared to state mixing.) The reason that the mixing of states leads to such an appreciable intensity for this forbidden double transition is that the EQQ interaction is of the same order of magnitude as the separation between the unperturbed states. This separation is 18, 11, and 6 cm^{-1} in H_2 , HD, and D_2 , respectively, so the double transition should be less intense in H_2 than in D_2 , in agreement with recent experiments.^{6,14} In H_2 , an accurate measurement of the intensity ratio $I[Q_1(0)+S_0(0)]/I[S_1(0)]$ is possible because the two components are well separated, and Barocchi *et al.* measured this ratio for solid para- H_2 pressurized to 244 bars, obtaining values ranging between 0.22 and 0.24. These experimental values agreed well with theoretical calculations when a value of 0.856 was used for ξ_{54} , the renormalizing parameter that relates the effective EQQ interaction to the interaction in the absence of zero-point motion.³⁴ Using this value for ξ_{54} and rescaling the parameter λ used in Ref. 14 for a zero pressure solid, the intensity ratio $I[Q_1(0)+S_0(0)]/I[S_1(0)]$ becomes 0.17. The measured value of 0.21 for HD is, therefore, in good qualitative agreement with the H_2 results. A straightforward application of the perturbation treatment used for H_2 in Ref. 14 is probably not really applicable to HD because of the smaller separation between the unperturbed

states.

A number of new features are observable between the $Q_1(0)$ and the $S_1(0)$ lines when the intensity scale is expanded, as shown in Fig. 5. To obtain frequencies and intensities of all of these features, the same procedure used in the rotational band was followed. After fitting the $Q_1(0)$ and $S_1(0)$ lines and subtracting these components plus a constant background, the remaining features were simultaneously fit to several components. The same Fano-type profile (4) used for the $R_0(0)$ line was used to fit the line labelled “?” because of its asymmetric shape and also in anticipation that it might be identified as the $R_1(0)$ transition, and Gaussians were used for the rest of the features. The results obtained for this line and the phonon band components are summarized in Table V. The feature labelled Q_R is the phonon sideband associated with the $Q_1(0)$ transition, and the separation between these two features is 59 cm^{-1} . The identity of the next peak adjacent to the Q_R phonon and labelled with a question mark is uncertain. It is tempting to identify this feature as the $R_1(0)$ transition, but this does not seem likely for several reasons. The most obvious objection is that this feature appears much broader than the $R_0(0)$ line. Furthermore, the frequency of this line was determined to be 3717.2 cm^{-1} , which is 7.5 cm^{-1} higher than the much more accurate value obtained for the $R_1(0)$ transition by McKellar and Clouter using a high-resolution FTIR spectrometer.¹⁸ This discrepancy falls well outside the estimated experimental uncertainty of $\pm 2\text{ cm}^{-1}$ and rules out the assignment of this line as $R_1(0)$, although a remeasurement of this line using higher resolution would be highly desirable. This feature does, however, share the same asymmetric Fano-type profile as the $R_0(0)$, and it is also accompanied by a more intense phonon band that appears to peak around 3780 cm^{-1} . To avoid confusion with the analogous phonon band in the rotational spectrum, this phonon has been labelled R_R^{vib} . The analogy with the rotational spectrum

TABLE V. Properties of the Q_R and R_R^{vib} phonon branches and the unidentified phonon features in the vibrational band determined from least-squares fitting. Two Gaussians were used to fit the Q_R and R_R^{vib} features. The intensity is given relative to the $S_0(0)$ transition.

Phonon branch components	Frequency (cm^{-1})	FWHM (cm^{-1})	Relative intensity
Q_R phonon:			
Q_R^a	3666.8	13	0.8×10^{-4}
Q_R^b	3685.0	27	3.8×10^{-4}
Q_R (total)	3681.2		4.7×10^{-4}
?	3716.9	12	1.2×10^{-4}
R_R^{vib} phonon:			
R_R^a	3765.9	27	2.0×10^{-4}
R_R^b	3783.4	19	1.9×10^{-3}
R_R (total)	3774.6		3.9×10^{-3}
Unknown feature	3824	52	7.0×10^{-4}

can be carried further: a small but distinct peak just to the right of the R_R^{vib} peak can be identified as the HD $Q_1(0) + D_2 S_0(0)$ double transition, which occurs in the same relative position as the much stronger $D_2 S_0(0)$ line, as can be seen from Fig. 2. Finally, like the HD $S_0(0)$ line, the $S_1(0)$ line appears to contain an additional component in its low-frequency wing, just to the high-frequency side of the double transition involving D_2 , giving the $S_1(0)$ line a slightly asymmetric appearance at its base.

The last feature included in Table V also currently remains unidentified. It is clearly analogous to the unidentified feature at 200 cm^{-1} in the rotational band. Both features were adequately modeled using a single Gaussian with a FWHM of 98 and 58 cm^{-1} in the rotational and vibrational bands. Given their extensive widths, both features certainly represent some type of lattice vibrational mode. It should also be pointed out that these features appear to be unique to HD; no asymmetry in the wing of the $S_0(0)$ line in H_2 was observed in Raman spectra recorded during these experiments, nor has anything similar occurring in H_2 or D_2 been reported in the literature. A tentative identification of this feature will be discussed in the following section.

V. DISCUSSION

Table VI presents a comparison of the measured integrated intensities of the new transitions that have been observed with the intensities calculated according to the theory outlined in Ref. 24. The theoretical values are those determined for a crystal oriented with its c axis aligned along the laboratory-fixed Z direction, although, as already pointed out, the samples were not single crystals but polycrystalline, and the possibility exists that the distribution of crystallite orientations was closer to being completely random. Therefore, the scattering intensities were also calculated for the case of a collection of randomly oriented crystals.²⁷ As it turns out, the scattering efficiencies for all but one of the Raman transitions considered are very nearly equal for the two extreme cases. Only the $U_v(0)$ transition is predicted to have a 10% larger scattering efficiency for the randomly oriented

TABLE VI. A comparison between the measured and theoretical intensities for the new Raman transitions observed in solid HD. All intensities are expressed relative to the $S_0(0)$ transition.

Transition	Measured intensity	Theoretical intensity
$R_0(0)$	$1.1 \pm 0.5 \times 10^{-4}$	1.6×10^{-4}
R_R	$4.2 \pm 2 \times 10^{-3}$	$2.6 \times 10^{-3\text{ a}}$
$T_0(0) + S_0(0)$	$4.4 \pm 1 \times 10^{-6}$	4.4×10^{-6}
$U_0(0)$	$6.2 \pm 0.6 \times 10^{-6}$	1.6×10^{-8}
$U_0(0) + S_0(0)$	$1.7 \pm 0.2 \times 10^{-5}$	6.7×10^{-8}
$R_1(0)$	$1.2 \pm 1 \times 10^{-4}$	4.8×10^{-6}
R_R^{vib}	$3.9 \pm 2 \times 10^{-3}$	

^aAttia *et al.*, Reference 24. This value strictly applies only for the case of $XY + XZ$ polarization.

case. The scattering intensity for the $R_0(0)$ transition shows the most sensitive dependence on the crystal orientation, with the scattered intensities varying in the ratios 2:0:1 for alignment of the c axis along the laboratory-fixed X , Y , and Z directions. For a completely random distribution of crystals, however, the intensity would be identical to that calculated for a single crystal oriented along the Z direction, as was assumed for these experiments.

The agreement between the measured and the theoretical intensities is very good for the $R_0(0)$ and the $T_0(0)+S_0(0)$ transitions. The disagreement for the $R_0(0)$ line is just outside the quoted experimental uncertainty, but this may well be an underestimate considering the difficulty inherent in separating a very weak, asymmetric line shape from an unknown background. Furthermore, according to calculations, the intensity of this line may vary between zero and twice the theoretical value given in Table VI, depending on the dominant orientation of the crystals. The agreement between measurement and theory for the $T_0(0)+S_0(0)$ line speaks for itself, and taken together with the $R_0(0)$ result, demonstrates that the theory of the interaction-induced polarizability described by Attia *et al.*²⁴ satisfactorily accounts for the intensities of these transitions, given the present experimental uncertainties.

The same thing cannot be said about the other zero-phonon transitions included in Table VI. In particular, the measured intensities of the $U_0(0)$ and the $U_0(0)+S_0(0)$ lines appear to be 300 to 400 times greater than the theoretical values. Clearly, the contribution from the interaction-induced polarizability to the intensity of these two transitions is negligible, and some other mechanism must be invoked to explain the appearance of these lines. It may be recalled that both transitions have been previously reported in solid H_2 and D_2 by Berkhout and Silvera.¹³ In contrast to HD, the interaction-induced polarizability makes no contribution to transitions involving $\Delta J=4$ in the homonuclear isotopomers. The only mechanism that contributes to these transitions in H_2 and D_2 , and probably the dominant mechanism in HD, is the mixing of rotational states differing by $\Delta J=2$ by the EQQ interaction. Further discussion of the mechanism responsible for the $U_0(0)$ and the $U_0(0)+S_0(0)$ transitions in solid HD will appear in another paper.

The measured intensity of the “?” feature in the vibrational band has been compared in Table VI to the theoretical value of the $R_1(0)$ transition. The measured value is 25 times greater than theory predicts; such a large discrepancy would not be expected given the fairly good agreement for the $R_0(0)$ transition in the rotational band. This large disagreement in intensities, taken together with the discrepancy of 7.2 cm^{-1} between the observed frequency and the previously measured position in absorption,¹⁸ definitely rules out the identification of this feature as the $R_1(0)$ transition. But what are the alternatives?

Another look at the most recent absorption spectrum of solid HD in the vibrational band¹⁸ shows the $R_1(0)$ line occurring in absorption, but it is very sharp (the

width of 2 cm^{-1} is much less than the measured value of 12 cm^{-1} quoted in Table V) and it occurs at the position of a sharp dip in the Q_R phonon branch. This dip at 3706 cm^{-1} in absorption seems to correspond with a similar minimum in the Raman spectrum of Fig. 5. As discussed by Zaidi³⁵ and by Bose and Poll,³⁶ this dip results from a strong coupling between the phonon states and the $J=1$ roton, and this coupling may be expected to influence the Raman spectrum as well. It is interesting to compare the observed structure in the Q_R phonon band with the richer structure seen in absorption,¹⁸ even though a difference in selection rules means a strict comparison cannot be made. The two components of the Q_R feature at 3667 and 3685 cm^{-1} correspond very closely with the two dominant peaks in the absorption spectrum at 3666.4 and 3689.7 cm^{-1} . Furthermore, the peak on the high-frequency side of the phonon dip in absorption occurs at 3722 cm^{-1} , which is only 5 cm^{-1} higher than the peak in the Raman spectrum that has been labelled “?” up to now. A tentative identification of this latter feature is that it represents the second peak in the Q_R phonon band, and that this phonon band has an interference dip that is very similar to the dip observed in absorption. The absence of an $R_1(0)$ line may be attributed to the weakness of the transition and insufficient resolution to resolve it from the phonon structure.

If this explanation of the feature at 3717 cm^{-1} is accepted, then it may appear strange that a significant phonon branch in the vibrational region (the R_R^{vib}) has been measured and yet the zero-phonon transition was too weak to be observed. Yet this apparent anomaly is supported at least qualitatively by the theoretical calculation of Attia *et al.* predicting an R_R phonon branch in the rotational band that is 15 times the intensity of the $R_0(0)$ line.²⁴ As pointed out by the previous authors, the intensities of the single molecule transitions such as $R_v(0)$ are reduced by the cancellation effect, which is a consequence of the hexagonal-close-packed (hcp) crystal structure of solid hydrogen. In fact, the R_R phonon branch was determined to have 38 times the $R_0(0)$ intensity, although no allowance was given for the two-phonon spectrum that is also expected to occur, so the discrepancy is not really as bad as it appears.

The identification of the unknown feature in the rotational band near 200 cm^{-1} as two-phonon scattering did not seem likely, and the occurrence of a similar feature in the vibrational band would seem to definitely rule this out. An alternative possibility is that this feature is a continuation of the R_R phonon band. Figure 6 offers some support for this hypothesis. The two fitted components of the R_R phonon band and the unknown feature are plotted separately on a horizontal scale that gives the frequency shift from the zero-phonon line. The top plot represents the rotational band and the middle plot the vibrational band. A comparison of these two plots with the bottom one, showing the three Q_R phonon band components and their separation from the $Q_1(0)$ line, reveals a pretty close correspondence between the separations of the three components from the zero-phonon transitions in all three plots. One problem with identifying the two

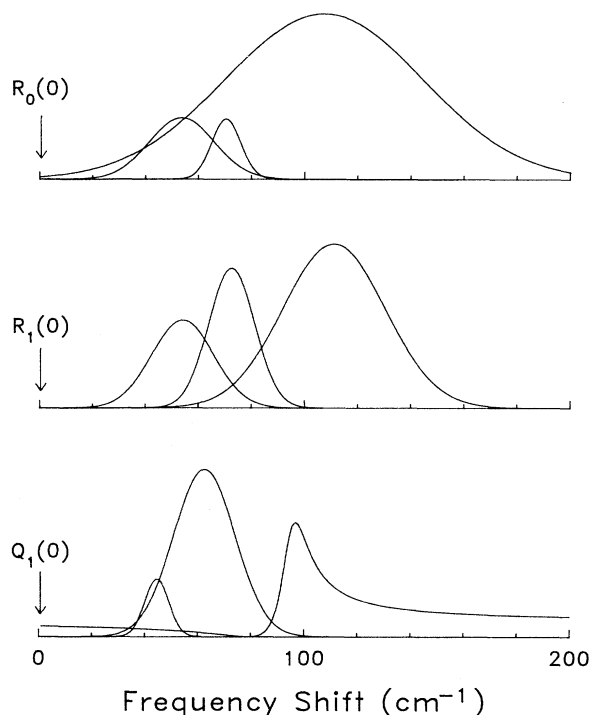


FIG. 6. A comparison between the three phonon branch components of the R_R , R_R^{vib} , and Q_R phonons. The horizontal scale gives the frequency shift from the zero-phonon frequency, indicated at zero on the horizontal axis. The intensities between the three different plots are not directly comparable.

unknown features as part of the R_R phonon bands is that it greatly increases the intensity of these phonons and therefore further magnifies the discrepancy with the theoretical values. For example, in the rotational band the total R_R intensity including the third component works out to be more than 300 times the intensity of the $R_0(0)$ line, while theory predicts a mere factor of 15. It appears that a more detailed theoretical study of the R_R phonons will be required before a definitive identification of the unknown features occurring in the rotational and vibrational bands can be made.

VI. CONCLUSIONS

The Raman spectrum of solid HD has been reexamined under high sensitivity using a conventional Raman spectrometer with an external resonating cavity. In the pure rotational band, an $R_0(0)$ line and a $T_0(0)+S_0(0)$ double transition were observed; the intensities relative to the allowed $S_0(0)$ transition were measured to be 1.1×10^{-4} and 4.4×10^{-6} , respectively. The agreement with the theoretical intensity for the double molecule transition was excellent, and given the uncertainty in the crystal orientation, the agreement for the $R_0(0)$ line was also very good. The $R_0(0)$ line was observed to have a Fano-type interference line shape, probably caused by coupling between the $J=1$ roton and the underlying

two-phonon continuum. It was impossible to observe the $R_0(0)+S_0(0)$ transition, whose relative intensity was calculated to be 1.2×10^{-4} , because of the strong $H_2 S_0(1)$ line that occurred in the spectrum at the same frequency.

A much more intense phonon band labelled R_R was also observed in the rotational band. This was a broad feature that was fit well using two or three Gaussian line shapes with center frequencies ranging from 42 to 71 cm^{-1} higher than the $R_0(0)$ frequency. The combined intensity of the R_R band was about 50% greater than the theoretical intensity, but there was no way of distinguishing this phonon band from the two-phonon scattering contribution that is expected to occur in the same frequency range.

A $U_0(0)$ line and a $U_0(0)+S_0(0)$ double transition were also observed in the rotational band. These transitions have been reportedly observed in solid H_2 and D_2 under high pressure,¹³ but in solid HD the $U_0(0)$ line does not overlap with the strong $S_0(1)+S_0(1)$ transition, as it does in H_2 and D_2 , so its identification in the solid HD spectra is much less ambiguous. Unlike the case of H_2 and D_2 , the interaction-induced polarizability, through the so-called "twice-shifted" polarizability coefficients, does contribute to the $U_0(0)$ and $U_0(0)+S_0(0)$ transitions in HD, but the calculated intensity was at least two orders of magnitude smaller than the observed intensity. Both transitions were accompanied by distinct phonon bands with intensities comparable to the zero-phonon lines.

The vibrational (0-1) band was also found to contain several features that have not been observed before. The $Q_1(0)+S_0(0)$ double transition was observed on the high-frequency side of the $S_1(0)$ line with an intensity of 0.21 relative to the total $S_1(0)+[Q_1(0)+S_0(0)]$ intensity. A wealth of new features were also seen between the $Q_1(0)$ and the $S_1(0)$ lines. A broad line with a Fano-type line shape at 3717 cm^{-1} occurred near the expected position of the $R_1(0)$ transition, but identification as this single molecule transition was not credible for two reasons. First, the frequency of the feature was 7 cm^{-1} higher than previous absorption measurements of the $R_1(0)$ line. Secondly, the measured intensity was 25 times greater than the calculated value, even though there was very good agreement between theory and experiment for the pure rotational $R_0(0)$ transition. An alternative explanation was that the feature at 3717 cm^{-1} was part of the Q_R phonon band accompanying the $Q_1(0)$ transition. The entire Q_R phonon band, consisting of a two-component feature with central frequencies of 3667 and 3685 cm^{-1} , a sharp dip in intensity near 3710 cm^{-1} , and a third feature at 3717 cm^{-1} , strongly resembled the Q_R phonon band observed in absorption spectra.

According to the calculated intensity, the $R_1(0)$ line should have been observable with the present sensitivity. Its absence may have been the result of insufficient resolution in the vibrational band. It would be of great interest to reexamine this spectral region under higher resolution to try and resolve this line from the broader Q_R phonon features.

Despite not being able to observe the zero-phonon

transition, a significant R_R^{vib} phonon band was observed consisting of at least two components with frequencies of 3766 and 3783 cm^{-1} . The appearance of this phonon band was very similar to the appearance of the R_R feature in the pure rotational band.

Finally, both the $S_0(0)$ and the $S_1(0)$ lines appeared noticeably asymmetric because of an additional feature in the low-frequency wings. After fitting both lines to a Lorentzian function, it was found that the two additional features could be well represented by a single Gaussian with a FWHM of between 50 and 100 cm^{-1} . The only tentative explanation for both features is that they are a continuation of the R_R phonon branches. With this identification, it was then shown that the structure of the R_R and the R_R^{vib} phonon bands were very similar to the Q_R phonon, with a two-component feature followed by a dip in the intensity, followed by a third component. The

only current difficulty with identifying the unknown features with the R_R phonon branches is that the total intensity of the phonons then becomes much greater, possibly by a factor of 20, than the theoretically predicted intensity.

ACKNOWLEDGMENTS

We gratefully acknowledge the helpful discussions and assistance with the theoretical calculations of Professor J. D. Poll and Professor R. H. Tipping, and the assistance of D. Tokaryk and J. Forrest with the experiments. T. Riddolls made the sample cell and also contributed to its final design. Financial support from the Natural Sciences and Engineering Research Council (NSERC) of Canada is also acknowledged.

-
- ¹G. Herzberg, *Spectra of Diatomic Molecules* (Van Nostrand, New York, 1950).
- ²P. W. Gibbs, C. G. Gray, J. L. Hunt, S. P. Reddy, R. H. Tipping, and K. S. Chang, *Phys. Rev. Lett.* **33**, 256 (1974).
- ³S. Paddi Reddy, A. Sen, and R. D. G. Prasad, *J. Chem. Phys.* **72**, 6102 (1980).
- ⁴R. D. G. Prasad, M. J. Clouter, and S. Paddi Reddy, *Phys. Rev. A* **17**, 1690 (1978).
- ⁵T. K. Balasubramanian, C.-H. Lien, K. Narahari Rao, and J. R. Gaines, *Phys. Rev. Lett.* **47**, 1277 (1981).
- ⁶S. B. Baliga, R. Sooryakumar, K. Narahari Rao, R. H. Tipping, and J. D. Poll, *Phys. Rev. B* **35**, 9766 (1987).
- ⁷M.-C. Chan and T. Oka, *J. Chem. Phys.* **93**, 979 (1990).
- ⁸K. Narahari Rao, *J. Mol. Struct.* **113**, 175 (1984).
- ⁹M. Okumura, M.-C. Chan, and T. Oka, *Phys. Rev. Lett.* **62**, 32 (1989).
- ¹⁰Man-Chor Chan, Szetsen Lee, Mitchio Okumura, and Takeshi Oka, *J. Chem. Phys.* **95**, 88 (1991).
- ¹¹M. Okumura, M.-C. Chan, and T. Oka, *Phys. Rev. Lett.* **62**, 32 (1989).
- ¹²W. R. C. Prior and E. J. Allin, *Can. J. Phys.* **51**, 405 (1973).
- ¹³P. J. Berkhout and I. F. Silvera, *Commun. Phys.* **2**, 109 (1977).
- ¹⁴F. Barocchi, A. Guasti, M. Zoppi, J. D. Poll, and R. H. Tipping, *Phys. Rev. B* **37**, 8377 (1988).
- ¹⁵R. A. Durie and G. Herzberg, *Can. J. Phys.* **38**, 806 (1960).
- ¹⁶M. Trefler, A. M. Cappel, and H. P. Gush, *Can. J. Phys.* **47**, 2115 (1969).
- ¹⁷Sang Young Lee, Sung-Ik Lee, J. R. Gaines, R. H. Tipping, and J. D. Poll, *Phys. Rev. B* **37**, 2357 (1988).
- ¹⁸A. R. W. McKellar and M. J. Clouter, *Can. J. Phys.* **68**, 422 (1990).
- ¹⁹R. H. Tipping and J. D. Poll, *Phys. Rev. B* **35**, 6699 (1987).
- ²⁰R. H. Tipping and J. D. Poll, in *Molecular Spectroscopy: Modern Research*, edited by K. Narahari Rao (Academic, Orlando, 1985), Vol. 3.
- ²¹J. D. Poll, R. H. Tipping, Sang Young Lee, Sung-Ik Lee, Tae W. Noh, and J. R. Gaines, *Phys. Rev. B* **39**, 11 372 (1989).
- ²²K. K. Lo, Ph.D. thesis, Ohio State University, 1983.
- ²³R. H. Tipping, Q. Ma, J. D. Poll, Tae W. Noh, Sang Young Lee, Sung-Ik Lee, and J. R. Gaines, *Phys. Rev. B* **38**, 6440 (1988).
- ²⁴M. Attia, M. Ali, R. H. Tipping, and J. D. Poll, *Phys. Rev. B* **40**, 8687 (1989).
- ²⁵I. F. Silvera, W. N. Hardy, and J. P. McTague, *Phys. Rev. B* **5**, 1578 (1972).
- ²⁶R. H. Tipping, J. D. Poll, and A. R. W. McKellar, *Can. J. Phys.* **56**, 75 (1978).
- ²⁷James J. Miller, Ph.D. thesis, University of Guelph, 1992.
- ²⁸J. J. Miller, R. L. Brooks, J. L. Hunt, and J. D. Poll, *Can. J. Phys.* **66**, 1025 (1988).
- ²⁹R. L. Brooks, S. K. Bose, J. L. Hunt, J. R. MacDonald, J. D. Poll, and J. C. Waddington, *Phys. Rev. B* **32**, 2478 (1985).
- ³⁰J. P. McTague, I. F. Silvera, and W. N. Hardy, in *Light Scattering in Solids*, edited by M. Balkanski (Flammarion, Paris, 1971), p. 456.
- ³¹U. Fano, *Phys. Rev.* **124**, 1866 (1961).
- ³²S. Y. Lee, Ph.D. thesis, Ohio State University, 1987.
- ³³S. S. Bhatnagar, E. J. Allin, and H. L. Welsh, *Can. J. Phys.* **40**, 9 (1962).
- ³⁴I. F. Silvera, *Rev. Mod. Phys.* **52**, 393 (1980).
- ³⁵H. R. Zaidi, *Can. J. Phys.* **48**, 1539 (1970).
- ³⁶S. K. Bose and J. D. Poll, *Can. J. Phys.* **65**, 1577 (1987).